Journal of Colloid and Interface Science 350 (2010) 305–314

Contents lists available at ScienceDirect

Journal of Colloid and Interface Science

www.elsevier.com/locate/jcis

Adsorption of copper on *Pseudomonas aureofaciens*: Protective role of surface exopolysaccharides

A.G. González [a], L.S. Shirokova [b,c], O.S. Pokrovsky [b,*], E.E. Emnova [d], R.E. Martínez [e], J.M. Santana-Casiano [a], M. González-Dávila [a], G.S. Pokrovski [b]

[a] Universidad de Las Palmas de Gran Canaria, Departamento de Química, Campus de Tafira, 35017 Las Palmas, Spain
[b] Géochimie et Biogéochimie Expérimentale, LMTG, Université de Toulouse, CNRS-IRD-OMP, 14 Avenue Edouard Belin, 31400 Toulouse, France
[c] Laboratory of Aquatic Ecosystems, Institute of Ecological Problems of the North, Russian Academy of Science Ural Branch Russian Academy of Science, Arkhangelsk, Russia
[d] Institute of Plant Genetics and Physiology, Moldavian Academy of Science, Padurii St., 26/1, MS-2002, Moldavia
[e] GeoForschungsZentrum Postdam, Section 4.1, Telegrafenberg, 14473 Postdam, Germany

ARTICLE INFO

Article history:
Received 7 April 2010
Accepted 9 June 2010
Available online 15 June 2010

Keywords:
Bacteria
Exopolysaccharide
Copper
Adsorption
Surface complexation

ABSTRACT

Adsorption of copper on exopolysaccharide (EPS)-rich and (EPS)-poor soil rhizospheric *Pseudomonas aureofaciens* cells was studied as a function of pH and copper concentration at different exposure time in order to assess the effect of cell exopolysaccharides on parameters of adsorption equilibria. The surface properties of bacteria were investigated as a function of pH and ionic strength using potentiometric acid–base titration and electrophoresis that permitted the assessment of the excess surface proton concentration and zeta-potential of the cells, respectively. For adsorption experiments, wide range of Cu concentration was investigated (0.1–375 μM) in order to probe both weak and strong binding sites at the surface. Experimental results were successively fitted using a Linear Programming Model approach. The groups with pK_a of 4.2–4.8 and from 5.2 to 7.2, tentatively assigned as carboxylates and phosphoryl respectively, are the most abundant at the surface and thus essentially contribute to the metal binding. The presence of exopolysaccharides on the surface decreases the amount of copper adsorbed on the bacterial cell wall apparently via screening the underlining functional groups of the cell wall. At the same time, dissolved EPS substances do not contribute to Cu binding in aqueous solution. Results of this study allow quantification of the role played by the surface EPS matrix as a protective barrier for metal adsorption on bacterial cell walls.

1. Introduction

Microorganisms have a high capacity of binding cationic metals onto their cell walls [1–8]. This process can control the mobility, speciation and bioavailability of metals in natural environments. Numerous studies have been conducted to address these issues, notably in the context of freshwater and saline environments [9,10], groundwaters [11,12], deep-sea hydrothermal systems [13,14], deep sedimentary basins [15,16] and sediments [17]. In addition, some physico-chemical research has been undertaken for marine and freshwater diatom species [18,19] spores of marine bacteria [20], freshwater algae [21], and whole bacteria and bacterial cell walls [6,22–28].

A common feature of many bacteria is the biosynthesis of extracellular polysaccharide (EPS) that can offer a protective barrier under environmental stress conditions [29]. In metal stress conditions, bacteria are highly stimulated to produce exopolysaccharides (EPS), which significantly increase the viability of cells exposed to metal-bearing solutions [30]. Commonly, exopolysaccharides are composed of glucose, fructose, manose, pyruvate and fucose, as well as mannuronic-and guluronic-acid complexes [31]. In addition, the EPS matrix comprises a mixture of heteropolysaccharides, proteins and nucleic acids [32,33]. Molecules of EPS from the majority of the bacterial species are negatively charged due to the presence of carboxyl and phosphoryl functional groups [34]. Carboxyl or hydroxyl groups are also known to be primarily involved in the metal-binding process by forming coordination bonds that facilitate the stability of ion polymer complexes [35].

Extracellular polysaccharides can bind toxic metal ions outside the cells, enabling organisms to ameliorate the presence of metal cations [36–39]. EPS may be considered as an efficient scavenger of heavy metals from water systems [40], thus reducing the concentration of free ionic metal activity [41]. EPS synthesis is affected by UV-radiation [42], dessication [43], and the presence of toxins [44]. However, the existing information contains certain contradictions/inconsistencies: on the one hand, EPS plays a role as a protective barrier of cell versus external metal load, and on the other

* Corresponding author. Fax: +33 561332650.
E-mail address: oleg@lmtg.obs-mip.fr (O.S. Pokrovsky).

0021-9797/$ - see front matter © 2010 Elsevier Inc. All rights reserved.
doi:10.1016/j.jcis.2010.06.020

hand, it is reported to adsorb significant amount of metal in the form of rather labile carboxylate or hydroxide complexes which may become easily bioavailable due to their location in the vicinity of cell membrane. To better address these contradictions, specially designed experiments for the same bacteria species, of similar cell wall composition, but different proportion of exopolysaccharides, would be necessary.

One of the most powerful tools able to characterize and predict metal interaction with bacterial cell walls and external envelopes is the thermodynamic approach. The thermodynamic description of interaction between microorganisms and aqueous solution often involves a surface complexation approach [6,20–23,26,45–49]. Surface speciation models allow rigorous description of reversible metal adsorption onto bacterial surface functional groups. This study represents a part of a concerted effort aimed at the expanding of the data base of adsorption parameters for aquatic and soil microorganisms with respect to metal pollutants. To achieve this goal, surface adsorption constants were measured for typical rhizospheric species *Pseudomonas aureofaciens* cultured in two different growth media that produced EPS-rich and EPS-poor cultures. This allowed quantifying the effect of EPS produced on the adsorption of copper by *P. aureofaciens* under rigorously constrained solution conditions.

The two specific questions addressed in this study are: (1) To what extent the abundant syntheses of EPS by bacteria modify metal adsorption parameters? (2) Are the charged (carboxyl-, phosphoryl-) groups in the cell wall screened by the EPS layers against aqueous Cu^{2+} or does soluble EPS complex copper ion in solution? Obtained results should allow better understanding of the effect of metal on bacterial growth through testing a link between the thermodynamic parameters of metal adsorption and the inhibition of culture growth.

2. Experimental

2.1. Culture characterization

The bacterial strain *P. aureofaciens* CNMN PsB-03 was obtained from the laboratory of Plant Mineral Nutrition and Hydric Regime (Institute of Genetics and Plant Physiology, Moldovan Academy of Sciences, Chisinau, Moldova). It was isolated from chernozem soil and selected due to its capacity to produce of exopolysaccharide (EPS) on a sucrose-containing medium [50].

The strain of *P. aureofaciens* was maintained at 4 °C in liquid succinic acid (SA) media [51], and cultured in two different media: (1) sucrose–peptone (SP) solution [52], thus promoting rich EPS synthesis which occurred in both Cu-free and Cu-rich media (up to 3 mM Cu^{2+}(aq)), or (2) SA media, yielding very poor EPS production. Cultivation was performed at 25 °C for 48–72 h with continuous shaking. The qualitative monosaccharide composition of the EPS produced in the indicated media was different: the SP-media yielded EPS composed of 76.1% fructose and 11.4% glucose, whereas the SA-media yielded EPS composed of 49.9% glucose, 22.3% fructose and 14% mannose [53]. Small amounts (<10% total sugars) of rhamnose, ribose, xylose and galactose were present in both EPS samples. Therefore, the most probable EPS for the SP-medium was the acidic polysaccharide levan (polyfructan). In contrast, glucan and some other heteropolymers were present in the SA-medium.

Experiments were undertaken for non-rinsed and rinsed bacterial biomass that produced two sub-samples for both EPS-rich and EPS-poor samples. In the first case, the bacteria were collected from the culture without rinsing, through centrifugation at 8000*g* for 20 mins. Therefore, for non-rinsed biomass, the EPS content of the cell wall was expected to remain intact. The rinsed biomass was produced by repeated centrifugation (three times) in an inert electrolyte solution ($NaNO_3$ or NaCl). Repetitive rinsing of biomass in electrolyte solution brings about the removal of part of the EPS from the cell surface. For the EPS-rich (SP-media) and the EPS-poor (SA-media) cultures, 28% and 6% total biomass were removed, respectively. The biomass concentration is given in g humid/L (centrifuged 20 min at 8000*g*). The conversion factor of wet to dry biomass was 3.6 and 5.0 for EPS-rich and EPS-poor cultures, respectively.

2.2. Infrared characterization of soluble exopolymers

The exopolymers (EP) were isolated from cell-free culture supernatant of both SP and SA media by precipitation with acetone (1:3, v/v) and dried at 40 °C. The infrared (IR) spectra of these products confirmed the presence of several functional groups [54]. The IR spectra of non-purified EP were recorded on Specord-74 spectrometer for spectral range 400–4000 cm^{-1} and the IR band identification was performed according to Bellamy [55]. The aliphatic functional groups (—CH_3, —CH_2, —C—H) were represented by absorption bands at 2960, 2850, 1465, 1370 cm^{-1}. The IR spectra showed absorption attributed to hydroxyl groups (O—H) at 3250 cm^{-1} (polymeric inter-molecular hydrogen bonds), 1070 and 1290 cm^{-1} (primary), 1100 cm^{-1} (secondary), 1140 cm^{-1} (tertiary). The IR absorption at 1086 cm^{-1} suggested the presence of ester bond C-O in EP molecules, which proved polysaccharide nature of tested exopolymers. The absorption bands at 715 and 525 cm^{-1}, confirmed the presence in EP chains of sulfur-containing groups (C—S or S—S). Moreover, protein groups (at 1540 and 1640 cm^{-1}) were present in all tested samples. The characteristic absorption signals for carboxyl groups (>C═O) were not detected in IR spectra of investigated EP samples synthesized by strain PsB-03 on both type of nutrient media. Note that, since infrared characterization was performed on EPS recovered from supernatants, this constitutes soluble EPS which has been shown to display rather less carboxyl groups relative to the bound EPS [56].

Subsequent investigations of EPS samples of *P. aureofaciens* PsB-03 using Brucker IFS88 FTIR spectrometer with MST detector supplied with IR ATR (Attenuated Total Reflection), included ZnSe element for 4000–700 cm^{-1} have shown the same results. The hydroxyl, aliphatic, ester, protein, sulfur-containing groups were detected, while the carboxyl groups (>C═O) were not revealed.

2.3. Electrophoretic measurements

The microelectrophoresis is a powerful technique to characterize the electric double layer (EDL) of microbial cell surfaces and their surface electric potential [57–62]. The zeta-potential of EPS-rich *P. aureofaciens* cultures were measured using a CAD Instrumentation "Zetaphorometer IV" Z 4000, microelectrophoremeter. The electrophoretic measurements were carried out in a quartz cell connecting two Pd electrode chambers. The cell was illuminated by a 2 mW He/Ne laser. During each measurement an electric field of 80 V/cm was applied in each direction. Metabolically active bacteria were suspended in 0.1 and 0.01 M $NaNO_3$ and pH was varied by adding 0.1 M HCl and NaOH in the range from 2.3 to 11 at 0.2 pH unit intervals. For each pH, three replicates of zeta-potential were performed.

2.4. Titration of bacterial surface

The acid–base titrations of bacteria cultured in SP and SA media were carried out in 0.1 M $NaNO_3$ at 25 ± 0.5 °C. After harvesting, bacterial biomass was rinsed three times with 0.1 M $NaNO_3$. The experiments were performed at constant biomass concentration of 10.0 g_{wet}/L. The suspension was pre-saturated with nitrogen

and first acidified using standardized 0.05 M HCl to initial pH of 3. The acid–base titration was done by adding small aliquots of NaOH (0.96 M) using an automatic titrator system Mettler® DL70 ES and continuous nitrogen bubbling. The addition interval was 0.1–0.4 pH units and the criteria of electrode potential stability between two subsequent additions was set as ⩽0.005 pH units/min. Note that this value is dramatically different from conventional 0.1 mV/s (∼0.1 pH units/min) used in most surface titrations of bacterial biomass.

The excess surface proton concentration was calculated from the equation [23,63]:

$$[H^+]_s = (C_{aj}\ (\text{suspension}) - C_{aj}\ (\text{reference})) - (C_{bj}\ (\text{suspension}) - C_{bj}\ (\text{reference})) \quad (1)$$

where C_{aj} and C_{bj} correspond to concentration of base and acid for the jth addition of titrant. As a reference system, the supernatant from the rinsed bacterial biomass was used and processed exactly in the same way as bacterial suspension. Note that this definition of excess surface proton concentration does not allow converting it directly to the cell surface charge, because the initial amount of surface protons is not known.

2.5. Metal adsorption

The copper adsorption experiments were designed to provide a quantitative characterization of metal binding by bacterial cells in a wide range of pH and Cu(II) concentrations in solution. For this, two types of experiments were carried out: (i) adsorption at constant initial metal concentration in solution as a function of pH (pH-dependent adsorption edge) and (ii) adsorption at constant pH as a function of metal concentration in solution (adsorption isotherm). All experiments were performed in the solutions undersaturated with respect to any copper oxide, hydroxide or carbonate phase as verified by speciation calculations with the MINTEQA2 computer code and corresponding database [64,65].

The initial copper concentration was always 5.2×10^{-5} M at variable pH and the copper concentration was varied between 0.44 and 375 μM at constant pH. The pH was adjusted by adding aliquots of NaOH (0.1 and 0.01 M) or HNO_3 (1, 0.1 and 0.01 M). pH was constant by adding MES (2-morpholinoethanesulfonic acid monohydrate) buffer, which was prepared at a concentration of 0.1 M and pH 5.5 and added to a final concentration of 0.005 M.

The adsorption of Cu^{2+} was followed as a function of time in series of kinetic experiments, performed at the initial concentration of 52 μM and pH 5.85. For this, EPS-rich bacteria were used as live (harvested at stationary stage), dead (autoclaved) and inactivated (0.01 M NaN_3 media). In addition, adsorption on live EPS-rich bacteria was studied as a function of pH and $[Cu^{2+}]_{aq}$ after 1 and 24 h of exposure time. All kinetic experiments were conducted in 0.1 M $NaNO_3$ under darkness with permanent stirring at a constant biomass concentration of 4 g_{wet}/L.

Most adsorption experiments were conducted during 1 h at 25 ± 0.2 °C in continuously agitated bacteria suspension with an ionic strength of 0.1 M $NaNO_3$ using 8 mL sterile polypropylene vials. Experimental conditions are listed in Table 1. The biomass concentration was kept constant at 4 g_{wet}/L and copper concentration in solution ($[Cu^{2+}]_{aq}$) ranged over four orders of magnitude from 0.13 μM to 4.72 mM (Table 1). This allowed proving not only abundant and weakly binding sites but also less abundant but much stronger binding sites. The pH was adjusted using aliquots of NaOH or HNO_3 and varied from 1.7 to 7.1 (Table 1). Live, freshly harvested (stationary stage) cells and dead (autoclaved) bacteria were used in the adsorption experiments.

To better account on the EPS presence on the cell surface, a number of experiments were carried out after rinsing the biomass to different degree. The biomass was centrifuged three times during 20 min at 5000g. The last supernatant was considered as a control and it was used for blank adsorption experiments in the absence of biomass. At the end of each experiment, the suspension was centrifuged at 4500g and the resulting supernatant was filtered through 0.45 μm acetate cellulose filter, acidified with ultrapure HNO_3 and stored in the refrigerator until the analysis. Adsorption of copper on cell walls for both EPS-rich and EPS-poor *P. aureofaciens* was investigated in the pH range between 1.7 and 6.8 (Fig. 1 and Table 1). The adsorption of copper on cell surface was quantified by subtracting, at each solution pH, the concentration of copper remaining in bacterial suspension from concentration of added copper in the supernatant (control experiments without biomass). The adsorption of copper on reactor walls at $2 \leqslant pH \leqslant 7$ was negligible (<10%). It was verified by blank (supernatant) experiments.

Reversibility of Cu^{2+} adsorption on live bacterial biomass was verified via treating the cells with adsorbed Cu after 1.5 h of exposure by 0.01 M EDTA during 10 min and analyzing Cu in the supernatant. This conventional method is widely used to distinguish

Table 1
List of experiments performed in this study and LPM model parameters for pH-dependent adsorption edge and constant-pH adsorption isotherm. All metal adsorption experiments were performed at 25 °C with 4 g_{wet}/L and 1 h of exposure time. All bacteria were rinsed in appropriate electrolyte solution except those indicated by ∗ (not rinsed). Some studies were carried out for 24 h of exposure time (∗∗).

Number	Type of experiment	Culture	Electrolyte	pH range	[Cu] range (μM)	pK_s/pK_m	Binding sites (mmol/g dry biomass)
EXP # 4	pH-edge	EPS-rich	0.1 M $NaNO_3$	1.66–5.58	52	−1.25	0.046
EXP # 5	pH-edge	EPS-poor	0.1 M $NaNO_3$	1.56–6.59	52	−1.75	0.052
EXP # 16	pH-edge	EPS-rich	0.1 M $NaNO_3$	1.64–6.95	52	−1.35	0.013
EXP # 17	pH-edge	EPS-rich∗∗	0.1 M $NaNO_3$	1.64–6.95	52	−1.20	0.017
EXP # 6	pH-edge	EPS-rich∗	0.1 M $NaNO_3$	2.99–6.25	52	−0.20	0.005
EXP # 7	pH-edge	EPS-poor∗	0.1 M $NaNO_3$	1.66–6.98	52	−0.90 and −0.25	0.006 and 0.004
EXP # 14-1	pH-edge	EPS-rich	0.1 M NaCl	1.72–6.48	52	−1.25 and 0.15	0.007 and 0.020
EXP # 8	Constant-pH isotherm	EPS-poor	0.1 M $NaNO_3$	5.51 ± 0.05	3–375	−0.60; 0.60; 2.30	0.043; 0.181; 0.756
EXP # 9	Constant-pH isotherm	EPS-rich	0.1 M $NaNO_3$	5.46 ± 0.02	3–375	−0.55 and 2.20	0.022 and 0.063
EXP # 11	Constant-pH isotherm	EPS-rich	0.1 M $NaNO_3$	5.19 ± 0.01	0.1–1.7	−0.40	0.068
EXP # 18	Constant-pH isotherm	EPS-rich	0.1 M $NaNO_3$	5.84 ± 0.02	472–4720	0.15	0.052
EXP # 19	Constant-pH isotherm	EPS-rich∗∗	0.1 M $NaNO_3$	5.84 ± 0.02	472–4720	0.25 and 1.70	0.042 and 0.020
EXP # 20	Constant-pH isotherm	Dead EPS-rich	0.1 M $NaNO_3$	5.85 ± 0.02	315–4720	−0.55 and 0.60	0.027 and 0.053
EXP # 21	Constant-pH isotherm	Dead EPS-rich∗∗	0.1 M $NaNO_3$	5.85 ± 0.02	315–4720	−0.95; 0.45; 1.61	0.020; 0.054; 0.011
EXP # 22	Constant-pH isotherm	EPS-poor	0.1 M $NaNO_3$	5.85 ± 0.02	157–4720	2.50	0.96
EXP # 23	Constant-pH isotherm	EPS-poor∗∗	0.1 M $NaNO_3$	5.85 ± 0.02	157–4720	0.25	0.143
EXP # 13	Constant-pH isotherm	EPS-rich	0.1 M NaCl	5.19 ± 0.01	0.3–1.7	−0.90	0.033
EXP # 15-1	Constant-pH isotherm	EPS-rich	0.1 M NaCl	5.17 ± 0.01	0.4–162	−1.55 and 1.30	0.005 and 0.153

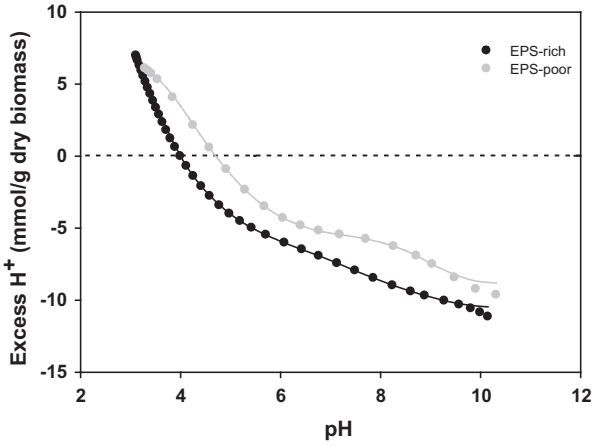

Fig. 1. Surface excess of protons with respect to initial hydrated bacterial surface of *Pseudomonas aureofaciens* in 0.1 M $NaNO_3$ at 25 °C. Circles are the experimental data for both culture media, EPS-rich and EPS-poor. Solid lines represent LPM fit to the data. Biomass concentration is 10 g_{wet}/L.

surface-adsorbed and intracellular-assimilated metal of algae and bacteria [66,67]. In all cases, very good recovery (>95%) of adsorbed copper was achieved, suggesting truly reversible surface adsorption process.

All filtered solutions were analyzed for aqueous Cu concentration using flame atomic absorption spectroscopy (Perkin Elmer 5100 PC spectrophotometer) with an uncertainty of ±2% and a detection limit of 0.05 mg L^{-1}, except the samples with low copper concentration which were analyzed using graphite atomic absorption spectroscopy (GF-AAS, Perkin Elmer AAnalyst 600) with a detection limit of 3 μgL^{-1} and an uncertainty of ±1%.

In order to study the Cu(II) speciation in solution, *in situ*, high-resolution potentiometry was used to monitor the activity and free concentration of Cu^{2+}(aq) in cell suspension. This method has been shown to be extremely effective in quantitative resolving metal adsorption constants as a function of pH and metal concentration in solution [i.e., 48,68–70]. Solid-contact Cu sulfide electrode (NIKO Analit®) coupled with Ag/AgCl reference electrode in 3.5 M KCl connected with solution via 1 M $NaNO_3$ salt bridge were calibrated at 4 < pH < 6 in standard $Cu(NO_3)_2$ solution. The efficiency of electrode response to the presence of only Cu^{2+} free (uncomplexed) metal was verified by adding strong Cu^{2+} complexants (EDTA, citrate) in the calibration solution. In all cases, adequate free Cu^{2+} concentration decreased in the presence of complexant, compatible with thermodynamic prediction of Cu^{2+} complexation with ligands. Similar results were obtained via monitoring of Cu^{2+} activity as a function of pH: a systematic decrease of the electrode potential due to $CuOH^+$ complexes formation at pH above 7–8 was observed. In the experiments with bacterial biomass, similar to previous work (i.e., Martinez and Ferris [48] and references therein), the electrode was fitted with sterile dialysis membrane (Spectra Por® 6, 6–8 kDa), which prevents fouling and oxidation of the ISE active surface by the bacterial cells and molecular oxygen, respectively. This membrane also prevented possible poisoning of electrode surface by extracellular substances with large molecular size. The constant ionic strength was maintained by adding 0.1 M $NaNO_3$. Potentiometric measurements were performed at 25 ± 0.5 °C in working concentration range of 10^{-5}–10^{-2} M with a detection limit of 10^{-6} M, and the uncertainty of 5%; a Nernstian slope of 29.1 ± 0.5 mV/pCu was obtained. Prior and after the measurements, the electrode was calibrated in cell supernatant solution having the same concentration of background electrolyte and bacterial exudates as the experimental solution.

Dissolved Organic carbon (DOC) concentration in solution was routinely monitored in all experiments of pH-dependent adsorption edge, at pH from 1.5 to 4.4, using a Carbon Total Analyzer (Shimadzu TOC-6000) with an uncertainty of 3% and a detection limit of 0.1 mg L^{-1}.

3. Results

3.1. Titration of bacterial surface and electrophoretic measurements

The surface titration experiments were carried out with rinsed EPS-rich and rinsed EPS-poor biomass in 0.1 M $NaNO_3$ for pH range from 3 to 10 (Fig. 1 and Table 2). Both types of cultures demonstrated high buffer capacity in the pH range from 5 to 10. The pH corresponding to zero excess proton adsorption was 4.0 ± 0.05 and 4.7 ± 0.11 for EPS-rich and EPS-poor bacteria, respectively (Fig. 1). This difference can be understood from the view point of EPS chemical composition: cells lacking in EPS should exhibit higher amount of positive charges, amine-like group of the cell surface envelopes, which are not protected by the exopolysaccharidic layer and having mostly neutral or negatively charged hydroxyl groups.

The electrophoretic experiments were carried out with EPS-rich and EPS-poor *P. aureofaciens* in 0.1 $NaNO_3$ (Fig. 2A). The value of pH isoelectric point (pH_{IEP}) is below 2 for both EPS-rich and EPS-poor cultures. The EPS-rich cells showed more negative mobility compared to EPS-poor cells in alkaline solutions (Fig. 2). This can be understood given a higher charge density in the EPS-rich cells, most likely linked to the high concentration of low pK_a sites (see Table 2 and the modeling section below) since the decrease of electrophoretic mobility started almost exactly at pH = pK_1. The chemical nature of these sites remains unknown. In addition to carboxylates/phosphodiester listed in Table 2, it could be also sulfate negatively charged groups. Another explanation could be the screening of positively-charged amine groups of the cell membrane by abundant hydroxylate moieties of the external EPS layers, as it was suggested for diatom cells (see for discussion Gélabert et al. [59]). The effect of ionic strength on bacterial zeta-potential was weakly pronounced (Fig. 2B), where the zeta-potential of EPS-rich cells, in 0.1 M and 0.01 M $NaNO_3$ was plotted as a function of pH. Note however, that further electrophoretic mobility measurements are necessary to assess the ionic strength dependence of the EPS-poor cells.

3.2. DOC and free copper concentration in the cell supernatant

The Dissolved Organic Carbon (DOC) was measured in the adsorption experiments as a function of pH at 1.5 < pH < 4.5 (Fig. 3). The DOC concentration was approximately 20 times higher

Table 2
Surface titration experiments and the LPM results. Experimental conditions: 25 °C, 10 g_{wet}/L, biomass rinsed with $NaNO_3$ 0.1 M three times, and pH between 3 and 10.

Cultures	pK_a	Binding sites (mmol/g dry biomass)	Possible functional group
EPS-rich	3.45	14.036	Carboxyl/phosphodiester
	4.75	1.4396	Carboxyl
	6.27	0.626	Phosphoryl
	7.15	1.231	Phosphoryl
	7.95	1.478	Amine
	9.10	1.126	Amine
EPS-poor	3.55	0.755	Carboxyl/phosphodiester
	4.15	4.324	Carboxyl
	5.20	3.713	Phosphoryl
	6.25	0.475	Phosphoryl
	7.60	0.361	Amine
	8.95	3.235	Amine

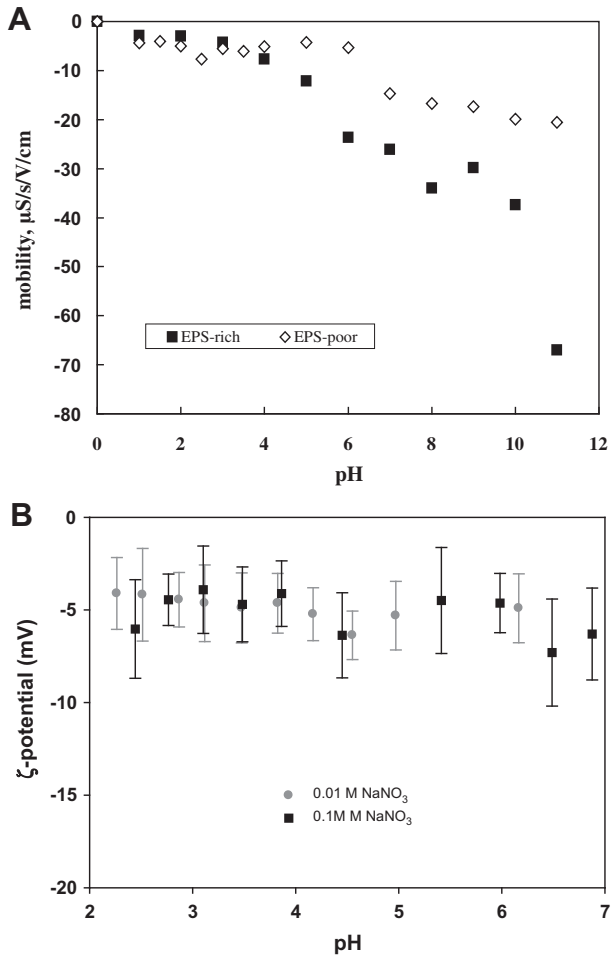

Fig. 2. (A) Electrophoretic mobilities of soil bacterial cells *Pseudomonas aureofaciens* in 0.01 M $NaNO_3$. (B) pH-dependence of EPS-rich *P. aureofaciens* zeta-potential at pH below 7 in 0.1 M and 0.01 M $NaNO_3$.

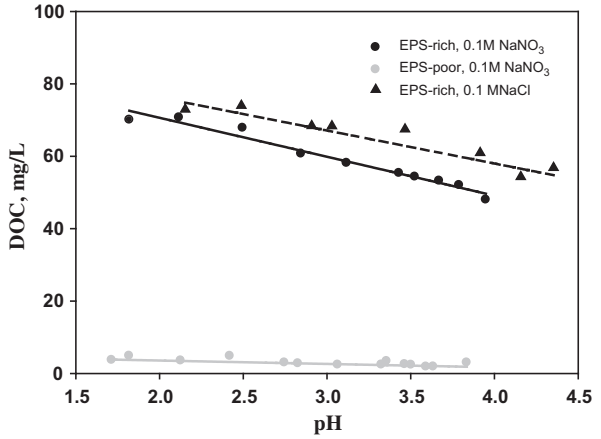

Fig. 3. Dissolved Organic Carbon (DOC) concentration as a function of pH during the metal adsorption experiments for *Pseudomonas aureofaciens* rinsed in different electrolyte solutions (0.1 M $NaNO_3$ and NaCl). Experimental conditions: 25 °C, 4 g_{wet}/L and 1 h of exposure time under darkness.

in EPS-rich cultures compared to the EPS-poor ones, consisting with much higher amount of EPS in the former. Some amount of this EPS can be released in solution in the course of the adsorption experiment. Several [DOC] measurements at 6 < pH < 8 yielded average values of 25 ± 5 and 5 ± 2 mg/L for EPS-rich and EPS-poor cultures, respectively. These values followed the trend shown in Fig. 3. The increase of [DOC] with decrease of pH is most likely to due to increase the EPS detachment/cells coagulation and surface layer degradation with increase of solution acidity. At the present time, we do not have a straightforward explanation for the higher [DOC] values in NaCl compared to $NaNO_3$.

The Dissolved Organic Carbon concentration was significantly higher in the experiments with EPS-rich *P. aureofaciens*. In order to study the role of DOC concentration in the solution and its capacity to complex copper, several experiments were carried out to measure free Cu^{2+} in cell supernatant solutions and in 0.1 M $NaNO_3$ using Cu^{2+}-selective electrode. Measuring free Cu^{2+} in EPS-rich and EPS-poor supernatants should help to distinguish the effect of Cu^{2+} complexation in solution and on cell surface. Plotted in Fig. 4 are the electrode potentials in the presence of various Cu^{2+} concentrations measured in 0.1 M $NaNO_3$ and in the EPS-rich and the EPS-poor media. There was approximately 2.1 ± 0.24 mV difference between the inert electrolyte (0.1 M $NaNO_3$) and the cell supernatant which signified that only 16 ± 2% of Cu^{2+} is bound in aqueous EPS complexes. However, free Cu^{2+} concentration was the same within ±5% in EPS-rich and EPS-poor supernatants. Thus no difference was detected for Cu^{2+} speciation in solution between two types of cultures. Therefore, the adsorption of Cu onto bacterial biomass was most likely controlled by the nature and abundance of cell surface groups, and not by soluble exopolymeric substances.

3.3. Adsorption of copper as a function of pH and copper concentration in solution

The pH-dependent adsorption edge for *P. aureofaciens* is illustrated in Fig. 5. Adsorption yield was always higher in bacteria subjected to rinse. The copper adsorption started at pH 2 and the maximum of adsorption was reached at pH 6.0 for both EPS-rich and EPS-poor cultures. Experiments on copper adsorption as a function of Cu concentration in solution were undertaken at constant pH of 5.5 with copper concentration varying between 0.13 µM and 4.72 mM (Fig. 6 and Table 1).

These experiments were carried out in both EPS-rich and EPS-poor *P. aureofaciens*. Similar to pH-dependent adsorption edge, the adsorption of copper at constant pH was higher for the EPS-poor culture compared to the EPS-rich culture. The slopes of dependence between $[Cu^{2+}]_{adsorbed}$ and $[Cu^{2+}]_{solution}$ in 0.01 M $NaNO_3$ were 1.06 ± 0.01 (r^2 = 0.99) and 0.94 ± 0.01 (r^2 = 0.99) for EPS-rich and EPS-poor cultures, respectively. These slopes were valid in the full range of metal concentration investigated. The slope was 0.75 in

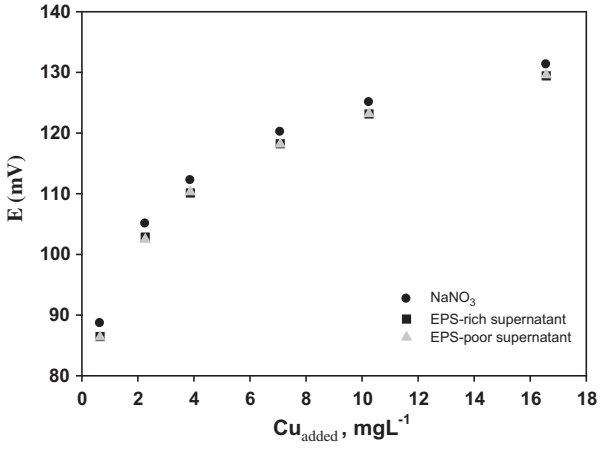

Fig. 4. Cu(II) free ion measured in solution using ion copper(II) selective in $NaNO_3$ 0.1 M and supernatants from EPS-rich and EPS-poor media at pH 6.

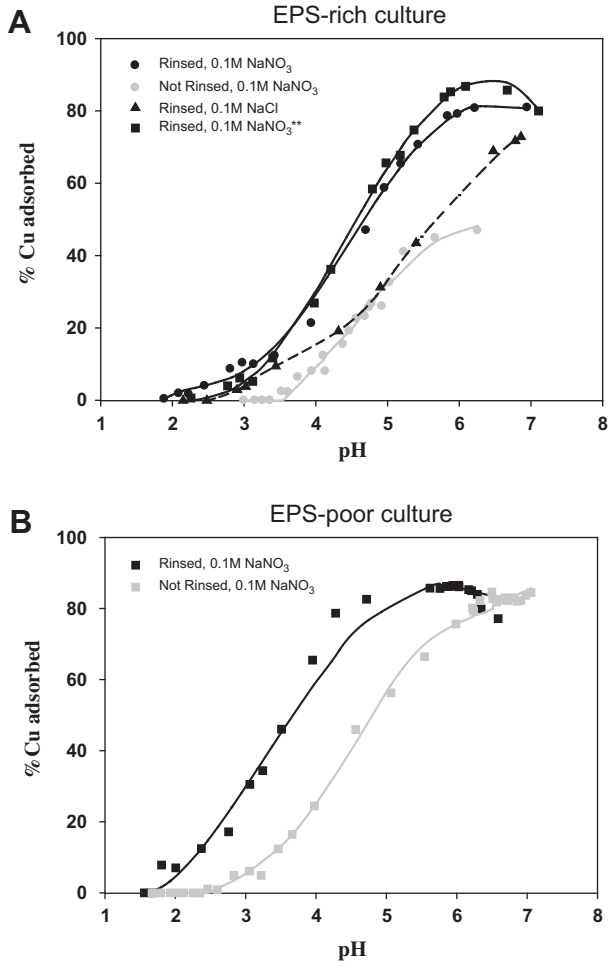

Fig. 5. Percentage of adsorbed copper as a function of pH for EPS-rich culture (A) and EPS-poor culture (B) of *Pseudomonas aureofaciens*. Solid line represents the result of LPM fit. Experimental conditions: 25 °C, 4 g_{wet}/L, 1 h exposure time under darkness, I = 0.1 M, [Cu]O = 52 μM. Some studies were carried out with 24 h (**) of exposure time.

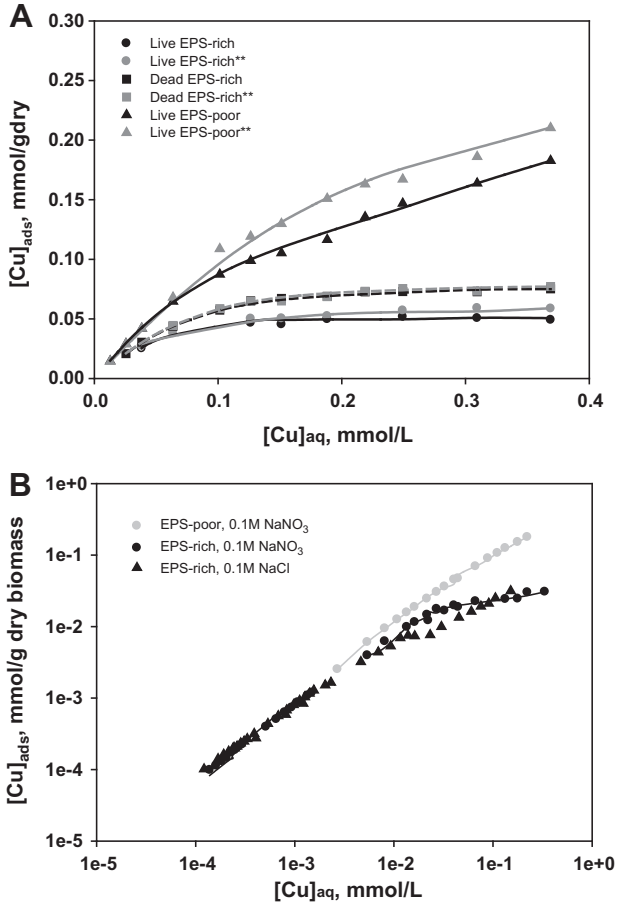

Fig. 6. Concentration of adsorbed copper as a function of copper concentration in solution (constant-pH adsorption isotherm) for *Pseudomonas aureofaciens* rinsed with electrolyte solutions ($NaNO_3$ and NaCl 0.1 M) in normal scale (A) and log-scale (B). Solid line represents the LPM fit. Experimental conditions: 25 °C, pH 5.5 ± 0.01, 4 g_{wet}/L and 1 h of exposure time under darkness. Some studies were carried out for 24 h of exposure time (**) and dead bacteria in 0.1 M $NaNO_3$.

the adsorption of copper in 0.1 M NaCl electrolyte solution and EPS-rich culture. It reflected some copper complexation with $Cl^-_{(aq)}$ which was explicitly taken into account during thermodynamic modeling.

Reversibility of Cu adsorption on live EPS-rich cultures was assessed at pH from 2.3 to 5.8. We found that, after 1.5 h of metal exposure to viable cells, between 2% and 13% of Cu was non-EDTA extractable, and the majority of the metal was reversibly adsorbed on the surface. These observations were consistent with results of the kinetic experiments demonstrating that the percentage of adsorbed Cu was practically constant (73 ± 4%) from 1 h to 24 h of exposure time (Fig. 7).

We did not find significant differences in adsorption yield between live and inactivated EPS-rich bacteria: the adsorption of copper(II) started at 45% and 37%, respectively after 1 min of exposure time, reaching the maximum at 20 h (77%) for both cultures. Bearing in mind that there were not significant differences in the adsorption yield for the EPS-rich cultures between 1 h and 24 h of exposure time (6% at pH 6, Fig. 5), our observations support neither significant efflux of copper from the interior of cells to the external solution nor the irreversible assimilation in the cell compartments. Only for EPS-poor cultures at high Cu loading, we observed some increase in the adsorption yield between 1 and 24 h exposure time (Fig. 6A). Although high-resolution kinetic data for EPS-poor culture were not available, this observation was consistent with a 10% increase in relative amount of adsorbed Cu for EPS-rich cultures within the same time interval (Fig. 7).

Noteworthy that there was a clear difference in the rate of Cu adsorption on dead bacteria, showing much faster achievement of a constant adsorption yield compared to the live biomass (Fig. 7). Most probably, this is linked to modified physical structure of heat-killed cells surface and complete removal of diffuse highly hydrated EPS layers after biomass autoclaving and extensive rinsing.

3.4. Linear programming modeling

Linear Programming Model approach (LPM) developed by Martinez et al. [23,48,49] was used to rationalize experimental results in order to obtain the main parameters of surface equilibria such as pK_s and pK_m of metal adsorption and pK_a of acid dissociation of *P. aureofaciens* cell surface functional groups. In contrast to simplified treatment of adsorption data using Langmuirian formalism used in previous study at high bacterial biomass/solution ratio (i.e., Pokrovsky et al. [28]), the present approach allows rigorous and much more realistic representation of continuum surface sites of cell surface polymers responsible for metal binding. The original code was modified in order to account for copper speciation in solution via calculating the percentage of free ion copper as a function of Cl^- concentration and pH taking into account Cl^- and OH^- complexation with Cu^{2+} using the stability constant from Ref. [65]. Linear

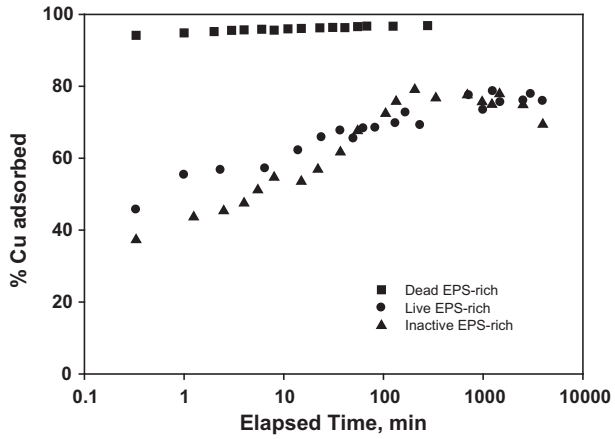

Fig. 7. Percentage of adsorbed Cu as a function of elapsed time for live, dead (autoclaved) and inactive (0.01 M NaN_3) bacteria in 0.1 M $NaNO_3$. Initial biomass was set constant at 4 g_{wet}/L and pH was fitted to 5.85. Initial Cu concentration was 52 μM.

programming regression techniques automatically minimize the number of binding sites and the absolute error, rather than the least squares. This approach finds one global minimum for the error function, which emphasizes zero as a possible solution and avoids convergence problems such as those found in FITEQL where the solution could be a local minimum [48]. Note that the LPM should be considered as a mathematical construction with no basis in true chemical nature of surface sites, as most surface complexation models. Indeed, the LPM uses a grid of fixed p$K_{s,j}$ values and optimizes parameters such as total binding site concentrations. Each site density, $[B_j]$, is assigned a positive value where zero is a possible result. This generates a p$K_{s,j}$ spectrum where discrete metal-binding sites are determined by the number of p$K_{s,j}$ values. In order to describe the interaction of metal cations (Me^{2+}) and protons with bacterial surface in pH-dependent adsorption edge experiments, a Me^{2+}/H^+ competition reaction, in Eq. (2) was assumed:

$$Me^{2+} + B_jH^0 \overset{K_{s,j}}{\leftrightarrow} MeB_j^+ + H^+ \tag{2}$$

where B_j represents a surface reactive site and $K_{s,j}$ the concentration apparent equilibrium constant conditional on ionic strength. For a jth deprotonated binding site at the ith pH value, $K_{s,j}$ can be defined as:

$$K_{s,j} = \frac{[MeB_j^+]_i \cdot [H^+]_{meas,i}}{[Me^{2+}]_{meas,i} \cdot [B_jH^0]_i} \tag{3}$$

In the above expression, $K_{s,j}$ is a function of experimentally determined proton and metal concentrations, ($[H^+]_{meas,i}$ and $[Me^{2+}]_{meas,i}$) and of the amount of Me^{2+} bound to the jth site at the ith pH value $[MeB_j^+]_i$.

For constant-pH adsorption isotherm data, the LPM model described earlier was modified to account for Me^{2+} binding as a function of increasing metal concentration. Therefore, reaction 2 is replaced by:

$$Me^{2+} + B_j^- \overset{K_m}{\leftrightarrow} MeB_j^+ \tag{4}$$

where B_j represents a specific surface functional group and $K_{m,j}$ the apparent metal–ligand binding constant conditional on ionic strength. For a jth deprotonated functional group at a fixed pH value, $K_{m,j}$ can be defined as:

$$K_{m,j} = \frac{[MeB_j^+]_i}{[Me^{2+}]_{meas,i} \cdot [B_j]_i} \tag{5}$$

In the above expression, $K_{m,j}$ is a function of experimentally metal concentrations, ($[Me^{2+}]_{meas,i}$) and of the amount of Me^{2+} bound to the jth site as a function of increasing biomass and a fixed pH value, $[MeB_j^+]_i$. Binding site concentrations will be calculated and assigned to a fixed p$K_{m,j}$ grid as explained previously for the pH-dependent adsorption experiments. The values of $K_{s,j}$ and $K_{m,j}$ found in this study for pH-edge and fixed pH metal complexation experiments are not directly comparable because K_s is a function of K_m, $K_s = K_m \times K_a$, where K_a is the acidity constant of a specific functional group on the bacterial surface. Therefore, the main shortcoming of this model is that the same proton adsorption sites constrained with the titrations are not used to constrain metal adsorption. However, we think that this may partially reflect the physical reality of the complex multilayer structure of the bacterial surface: the gelatinous EPS layer might slow down the diffusion rate of the copper ion into the cell wall chelating matrix where as this diffusion barrier for protons should be much smaller.

Results of the model fit to adsorption experiments are shown as solid lines in Figs. 1, 5 and 6 and the model parameters are illustrated in Table 1 and 2. The pK_s values were calculated from the pH-dependent adsorption edges (Table 1). The amount of available sites capable of binding copper varied from 0.01 to 0.05 mmol/g_{dry}. The higher negative magnitude of the pK_s, the stronger the binding capacity of the each functional group on bacterial surface [49]. Thus, the most important and negative pK_s value (−1.75) corresponded to EPS-poor culture grown on SA media (Exp # 5), for which the concentration of available sites was also high, 0.052 mmol/g dry biomass. Consequently, the concentration of available sites was lower for the EPS-rich culture (Exp # 1, 0.046 mmol/g dry biomass) and the stability of surface binding groups was lower (pK_s = −1.25) than the EPS-poor strain (pK_s = −1.75).

The pK_m values were obtained from the adsorption experiments as a function of metal aqueous concentration at constant pH (Fig. 6). Results were presented in Table 1. The amount of total metal sites available for metal adsorption ranges from 0.01 to 0.96 mmol/g dry biomass. As for pH-dependent adsorption edge, the highest number of surface binding sites occurred in the EPS-poor culture (0.96 mmol/g dry biomass and pK_m = 2.5), which was about one order of magnitude higher than for the EPS-rich culture at similar conditions. Dead bacteria yielded total amount of copper binding sites (0.080 and 0.085 mmol/g_{dry}, Exp # 20 and 21, respectively) which was comparable to EPS-rich live bacteria (0.05–0.08 mmol/g_{dry}, Exp # 9, 11, 18, 19, Table 1). Therefore, although the adsorption was much faster on dead bacteria (Fig. 7), the number of sites capable of binding metals was quite similar.

4. Discussion

Bacteria cell walls play a dominant role in the metal scavenging by microorganisms because various functional groups of the cell wall display a strong affinity for metal cations. With pH increase, these groups are progressively deprotonated forming anionic ligands capable of binding metals [47]. Results of this work demonstrated that adsorption of copper was higher by bacteria subjected to rinsing compared to those having their EPS envelopes intact. For example, non-rinsed bacteria exhibited the maximal adsorption yield of 70% versus 80% for 0.1 M $NaNO_3$-rinsed cultures (Fig. 5). The repetitive rinsing of bacteria removed external exopolysaccharidic layer and allowed to reactive functional groups of cell wall to interact with aqueous solution. The effect of rinsing was much

more pronounced for EPS-rich cultures where the loss of biomass was more important (28% and 6% for EPS-rich and EPS-poor media, respectively). Therefore, irrespective of the difference in chemical composition of cell walls for two subcultures that may stem from cell growing in SP and SA media, removing the EPS clearly increased the adsorption capacity of the total biomass *P. aureofaciens* with respect to Cu^{2+}. At the same time, the relative change in adsorption yield after cell rinsing (e.g., ~1/3 at pH 4, see Fig. 5) had similar magnitude for both EPS-rich and EPS-poor cultures. Apparently, the rinsing of bacteria brought about removal of similar relative proportion of the cell surface EPS layers because the physical nature of the EPS and the degree of the EPS attachment to the cell surface were similar among two subcultures.

Note that although the bulk of existing information on the cells-EPS-metal interaction demonstrates increasing capacity of metal adsorption on bacteria in the presence of EPS (see Refs. [71,72] and references therein], some previous studies indicated weak or even negative effect of bacterial EPS on metal adsorption. In particularly, Tourney et al. [73] demonstrated that the EPS removal does not affect the metal adsorption capacity of *Bacillus licheniformis* as the concentration of main binding sites, carboxyl and phosphate functional groups, was only slightly affected by EPS extraction. Moreover, macroscopic adsorption and FTIR analysis indicated that the EPS layer did not significantly enhance Cd binding to *Pseudomonas putida* [30] and in some cases, the EPS layer demonstrated a lower affinity for metal binding than the isolated cell walls [74]. Tourney et al. [73] proposed two possible explanation for these findings of weak effect of EPS on metal binding. First, the EPS production is known to induce a considerable degree of cell aggregation in suspension, which is likely to reduce the surface area available for metal adsorption. Second, the release of large quantities of DOC from EPS layer may complex metal in solution, in competition to cell walls. Our potentiometric measurements (Fig. 4) unequivocally demonstrated the absence of Cu^{2+} complexation with external EPS of *P. aureofaciens* and as such we submit that the EPS for this bacterium can be considered simply as an outer envelope shielding the cell surface from metal exposure, a hypothesis firstly suggested by Touney et al. [73].

The experimental results for pH-dependent adsorption edge were properly fitted using Linear Programming Model approach. This model is convenient for studied complex 3-D multiple layer system having both EPS component and rigid bacterial cell walls [23,63,75]. Note that, because the binding to EPS was weak and the effect of background electrolyte on surface potential was not pronounced, the Donnan shell-like model was not necessary. Other work used electrostatic approaches such as the constant capacitance model converged to three sites [25,76] whereas non-electrostatic models tend to consider four surfaces sites [77] and more suitable for describing ESP-bearing bacteria [78]. The highest log K_s (−1.75) was obtained for EPS-poor cultures produced in SA-media (Exp # 5). Results of the copper adsorption on *P. aureofaciens* at constant pH experiments and variable copper concentration also demonstrated higher adsorption yield for the EPS-poor cultures. Overall, the LPM parameters extracted from experimental data showed an order of magnitude higher adsorption site densities for the EPS-poor cultures compared to the EPS-rich cultures (Exp # 8, 22 and 9, 18 of Table 1).

Measurements of Cu speciation in solution using Cu^{2+}-selective electrode did not reveal any difference in Cu complexation with soluble exopolymers from EPS-rich and EPS-poor cultures having drastically different dissolved organic matter concentrations (Figs. 3 and 4). Therefore, adsorption of Cu on bacterial biomass is most likely controlled by the nature and abundance of cell surface groups, and not by soluble exopolymeric substances. It can be hypothesized that the weaker adsorption of Cu on the surface of EPS-rich cultures is due to screening (protection) of metal-binding internal moieties (possible carboxylate having pK_a of 4.2–4.8, and phosphoryl with pK_a of 5.2–7.2, of the cell wall and membrane) by rather inert EPS layers having mostly hydroxyl, aliphatic and ester groups with very small amount of carboxylates as revealed by FTIR investigation. Our previous study of adsorbed Cu chemical status via EXAFS spectroscopy demonstrated essentially carboxylate binding of Cu(II) on the surface of both EPS-rich and EPS-poor cultures, although rigorous distinguishing between surface carboxylate and phosphorylate was not possible [27].

Like for many aquatic microorganism surfaces [26,58,59,79] we observe, for *P. aureofaciens*, an apparent discrepancy between the pH of isoelectric point measured by electrophoresis ($pH_{IEP} < 2.5$) and pH of zero excess surface proton adsorption assessed by surface titration (between 4 and 5). This difference may stem from the uncertainty of definition of zero proton adsorption at the initial (reference) state of the cells prior to titration. Note however that other surface charged groups, such as sulfate or metal-linked pyruvyl groups, like in cyanobacteria (e.g., Refs. [80,81]), not probed by surface titration in the pH range of 3–10, can be responsible for negative zeta-potential even in highly acidic solutions and as a result, the "$[H^+]_{initial}$ condition is not zero. Unfortunately, because the pH_{IEP} of *P. aureofaciens* could not be measured, correction of the titration curve from "proton excess" to "proton balance" is not possible. The second possible explanation of the discrepancy between results of electrophoretic mobilities and surface titration lies in the multilayer surface structure of microorganisms: the cell wall proteins bearing amine moieties are covered by most external layer having essentially carboxylate-like groups. Apparently, for *P. aureofaciens*, despite the presence of thick, but relatively inert EPS envelopes, reversible protonation/deprotonation of internally located amine groups from peptidoglycan and proteins of the cell wall is responsible for the high concentration of surface proton excess measured during titration experiments (Fig. 1). These amine groups are situated far from the shear plane and thus cannot contribute to the zeta-potential development. In contrast, the weak amount of dissociated > R-COO^- groups on the surface (pK ~ 4) even at pH 2 is sufficient to provide a negative zeta-potential. Similar explanation has been recently proposed for the difference in pH_{PZC} and pH_{IEP} of another gram-negative bacterium, *Shewanella oneidensis* [72].

Our results also demonstrate that the effect of ionic strength on zeta-potential of EPS-rich culture is rather small and poorly pronounced (Fig. 2B). This observation can be accounted for the presence of diffuse 3-D highly porous EPS layer of rhizospheric bacteria. Due to this spatial organization, protonation/deprotonation of functional groups at the cell envelopes occurs at the distance from the shear plane that is much larger than that for individual cells or inorganic particles. As a result, large ions of background electrolyte do not sufficiently approach the charged surface and thus weakly contribute to potential at the shear plane. A weak effect of ionic strength on electrophoretic mobility of EPS-rich *B. licheniformis* observed in the range of 0.1–0.001 M has been explained by the contraction of the EPS layer with ionic strength [78]. Therefore, it is possible that the change in charge density associated with swelling of the EPS envelope at low ionic strength, which would compensate for charge-shielding [82] can be responsible for independence of electrophoretic mobilities of *P. aureofaciens* on ionic strength, observed in the present study.

Results of potentiometric surface titration allowed constraining stability constants of the acid–base protonation reactions controlling the buffering capacity of bacterial surfaces (Table 2). Resulted pK_a values can be separated in four groups: ≈3.5, 4–5, 5–7 and 8–10. In accordance with previous studies [23,26,73,76,83,84], they can be identified as carboxyl/phosphodiester, carboxylate, phosphoryl, and amine, respectively. Note that the chemical nature of surface sites listed in Table 2 cannot be assessed solely from surface

titration without spectroscopic characterization and as such it should be considered as tentative, hypothetical assignment. Other recent works found similar sites presenting on bacterial surfaces at pH from 3 to 9 [77,83–85]. Results of surface titration modeling demonstrated that the groups with pK_a = 4.15–4.75 (probably carboxylates) are the most abundant moieties constituting 78% and 40% of total available sites in individual EPS-rich and EPS-poor cultures, respectively. Since the possible phosphoryl groups (pK_a = 5–7) having higher affinity to proton (and, thus, metal) were more abundant in the EPS-poor bacteria (4.2 mmol/g dry and 1.9 mmol/g dry for EPS-poor and EPS-rich cultures, respectively), the Cu binding is also stronger for EPS-poor *P. aureofaciens*. Analysis of available literature data demonstrates that the role of EPS in bacterial cell surface charge development is rather contradictory. Ha et al. [72] concluded that the EPS-free strain of *S. oneidensis* has decreased proton binding capacity and lower participation of carboxyl and amine functional groups in proton binding, whereas the opposite is true for phosphoryl groups. Similar conclusion on lower concentration of amide and carboxyl functional groups in EPS-free cultures has been reached for *B. licheniformis* [84]. In contrast, Tsuneda et al. [86] found that the presence of an EPS layer on bacterial cells decreased the charge density and hence led to a lower electrophoretic mobility compared to ESP-free cells. Moreover, it has been shown both from potentiometric titration and electrophoretic mobility that the sheath materials of cyanobacteria *Calothrix* have a lower charge density compared to the exposed cell wall [24]. Most likely, the EPS composition and physico-chemical properties are linked to the nature and the lifestyle of EPS-producing microorganism and as such may significantly vary among different groups and different strain of bacteria. The specificity of *P. aureofaciens* is further confirmed by the observation of very weak complexation of soluble EPS with Cu^{2+} in aqueous solution (Fig. 4) whereas other gram-negative bacteria are known to complex metals by EPS [87].

Noteworthy that the concentration of available sites capable to adsorb protons and hydroxyls at the EPS-poor *P. aureofaciens* cell surface (0.4–4 mmol/g dry biomass, Table 2), are of the same order of magnitude than reported for other bacteria such as *B. subtilis* and *E. coli* [23], bacterial consortia [77], marine diatoms and freshwater periphytic species [88], and cyanobacteria [26]. This range is also consistent with recent results of Lamelas et al. [70] on EPS extracted from gram-negative bacteria (0.89–1.62 mmol/g dry). These points out on the similarity of proton- and metal-binding properties between soil rhizospheric and aquatic microorganisms stemming from similar molecular mechanisms involved in passive interaction of cell wall with aquatic metal cations. Further structural spectroscopic information is therefore needed to distinguish between different types of functional groups controlling metal binding at the surface. Note an important difference between the number of proton available site numbers inferred from acid–base titration (Table 2) and Cu-binding sites calculated from Langmuirian adsorption isotherm and pH-dependent adsorption edge (Table 1). This may reflect the poor availability of surface metal-binding moieties for aqueous metal ions; it is possible that diffusion of large-size cations such as $Cu^{2+}_{(aq)}$ in the external protective EPS layer around the cell is much slower than that of protons/hydroxyls. Another possibility of lower Cu adsorption onto the surfaces on unwashed EPS-rich bacteria, compared to EPS-poor culture, is the presence of surface adsorbed Ca or Mg from the growth media, as it was reported for other bacteria [26,47]. However, this mechanism is unlikely to operate for *P. aureofaciens* because our adsorption/desorption experiments: (1) did not reveal any significant Mg^{2+} and Ca^{2+} binding to bacterial cell wall; (2) demonstrated only weak proportion of surface sites occupied by Mg and Ca, by a factor of 10–100 smaller than the amount of Cu-binding sites and (3) confirmed significantly higher Cu adsorption density of EPS-poor cells compared to EPS-rich cells, after extensive treatment of the biomass by EDTA to remove surface Ca and Mg. This is described in details in the Electronic Annex (Appendix A).

With regard to metal toxicity, results of the present work on soil rhizospheric bacteria *P. aureofaciens* growing in Cu-amended soils [54] do not allow direct assessment of cell protection mechanism from the metal pollution since the EPS is produced to the same extent regardless of whether or not there is Cu in the media and special toxicological tests are necessary to better understand the role of EPS on cell viability. However, it follows that the development of thick EPS layer decreases the availability of aqueous copper to surface reaction centers of the cell wall and this, presumably, may decrease the intracellular metal assimilation. Compared to most other studied bacteria, the EPS production by *P. aureofaciens* does not contribute to complexation of aqueous ions Cu^{2+} while prevents the metal adsorption on the cell surface. In the wide range of metal concentration studied in this work (0.1–375 μM), the strong binding sites such as sulfhydryl moieties are not evidenced from macroscopic physico-chemical treatment of adsorption equilibrium. Further *in situ* spectroscopic techniques are necessary to reveal the true heterogeneity of surface sites and the change of Cu speciation upon its translocation from the surface layer to the interior of the cell.

5. Conclusions

The presence of exopolysaccharides on the cell walls of *P. aureofaciens* decreased the adsorption of copper via screening the cell surface reactive centers by relatively chemically inert polysaccharidic layer. This was observed during adsorption experiments performed on EPS-poor and EPS-rich cultures of the same species as a function of pH and copper concentration in solution. The external EPS do not possess significant amount of metal-binding centers being composed mainly of hydroxyl, ester, and aliphatic components. As such, they present a physical (diffusion) barrier for metal ion to approach reactive surface sites of the cell wall. Acid–base titration and electrophoretic measurements of *P. aureofaciens* revealed the presence of groups having pK_a in the range of 3.5, 4.2–4.8, 5.2–7.2, and 7.6–9.1 which may tentatively correspond to carboxyl, phosphodiester, phosphoryl and amine moieties as the main surface functional groups capable of proton- and metal-binding. Concentration of Dissolved Organic Carbon was significantly higher in experiments with EPS-rich culture compared to those with EPS-poor culture. The complexation of Cu^{2+} with exopolymeric substances in aqueous solution was very weak and similar between two types of cultures as confirmed by $Cu^{2+}_{(aq)}$ activity measurement via Cu^{2+}-selective electrode. Therefore, the main mechanism of *P. aureofaciens* cell protection from toxic metal stems from screening of strongly-binding functional groups of the cell wall such as phosphoryl (pK_a = 5.2–7.2) by abundant exopolysaccharides of the most surface layers.

Acknowledgments

The authors are grateful to two anonymous reviewers whose insightful comments allowed significant improvement of the manuscript. This work has been supported by the PICASO project (HF2006-0161); Acción Integrada Hispano-Francesa and the PhD grant for A. González (BES-2007-15776) associated to the project CTM2006-09857 from the Spanish Ministerio de Ciencia y Tecnología. Support of LEA "LEAGE", ANR Re-SYST and EC2CO program are equally acknowledged. Mr. Gordon Hamilton post-edited the English style.

Appendix A. Supplementary material

Supplementary data associated with this article can be found, in the online version, at doi:10.1016/j.jcis.2010.06.020.

References

[1] T.J. Beveridge, R.G.E. Murray, J. Bacteriol. 141 (1980) 876.
[2] M.L.S. Gonçalves, L. Sigg, M. Reutlinger, W. Stumm, Sci. Total Environ. 60 (1987) 105.
[3] T.J. Beveridge, Annu. Rev. Microbiol. 43 (1989) 147.
[4] M. Ledin, C. Drantz-Rulcker, R. Allard, Soil Biol. Biochem. 28 (1996) 791.
[5] S.M. Barns, S.A. Nierzwicki-Bauer, in: J.F. Banfield, K.H. Nealson (Eds.), Rev. Mineral. Min. Soc. Am. 35 (1997) 35.
[6] J.B. Fein, C.J. Daughney, N. Yee, T. Davis, Geochim. Cosmochim. Acta 61 (1997) 3319.
[7] M. Ledin, C. Drantz-Rulcker, R. Allard, Soil Biol. Biochem. 31 (1999) 1639.
[8] S.C. Wu, Y.M. Luo, K.C. Cheung, M.H. Wong, Environ. Pollut. 144 (2006) 765.
[9] G.G. Geesey, W.T. Richardson, H.G. Yeomans, R.T. Irvin, J.W. Costerton, Can. J. Microbiol. 23 (1997) 1733.
[10] R.W. Harvey, L.W. Lion, L.Y. Young, J.O. Leckie, J. Mar. Res. 40 (1982) 1201.
[11] S.K. Mahmood, R.P. Rama, Bull. Environ. Contam. Toxicol. 50 (1993) 486.
[12] M.Y. Corapcioglu, S. Kim, Water Resour. Res. 31 (1995) 2639.
[13] K.W. Mandernack, B.M. Tebo, Geochim. Cosmochim. Acta 57 (1993) 3907.
[14] E.T. Baker, R.A. Freely, M.J. Mottl, F.T. Sansone, C.G. Wheat, J.A. Resing, J.E. Lupton, Earth Planet. Sci. Lett. 128 (1994) 1.
[15] W.C. Ghiorse, F.J. Wobber, in: Deep Subsurface Microbiology Geomicrobiol. J., vol. 7, Crane, Russak, New York, 1989, p. 130.
[16] M.M. Yakimov, K.N. Timmis, V. Wray, H.L. Fredrickson, Appl. Environ. Microbiol. 61 (1995) 1706.
[17] D. Borrok, B.F. Turner, J.B. Fein, Am. J. Sci. 305 (2005) 826.
[18] M. González-Dávila, J.M. Santana-Casiano, J. Perez-Peña, F.J. Millero, Environ. Sci. Technol. 29 (1995) 289.
[19] M. González-Dávila, J.M. Santana-Casiano, L.M. Laglera, Mar. Chem. 70 (2000) 1129.
[20] L.M. He, B.M. Tebo, Appl. Environ. Microbiol. 64 (1998) 1123.
[21] H.B. Xue, W. Stumm, L. Sigg, Water Res. 22 (1988) 917.
[22] A.C.C. Plette, W.H. Van Reimsdijk, M.F. Bendetti, A. Van der Wal, J. Colloid Interface Sci. 173 (1995) 354.
[23] R.E. Martinez, D.S. Smith, E. Kulczycki, F.G. Ferris, J. Colloid Interface Sci. 253 (2002) 130.
[24] V.R. Phoenix, R.E. Martinez, K.O. Konhauser, F.G. Ferris, Appl. Environ. Microbiol. 68 (2002) 4827.
[25] B.T. Ngwenya, I.W. Suthermand, L. Kennedy, Appl. Geochem. 18 (2003) 527.
[26] O.S. Pokrovsky, R.E. Martinez, S.V. Golubev, E.I. Kompantseva, L.S. Shirokova, Appl. Geochem. 23 (2008) 2574.
[27] O.S. Pokrovsky, G.S. Pokrovski, L.S. Shirokova, E.E. Emnova, Geophysical Research Abstracts, vol. 10, 2008. EGU2008-A-01768, 2008. SRef-ID: 1607-7962/gra/EGU2008-A-01768.
[28] O.S. Pokrovsky, J. Viers, E.E. Emnova, E.I. Kompantseva, R. Freydier, Geochim. Cosmochim. Acta 72 (2008) 1742.
[29] S.K. Kazy, P. Sar, S.P. Singh, A.K. Sen, S.F. D'Souza, World J. Microbiol. Biotechnol. 18 (2002) 583.
[30] M. Ueshima, B.R. Ginn, E.A. Haack, J.E.S. Szymanowski, J.B. Fein, Geochim. Cosmochim. Acta 72 (2008) 5885.
[31] J.F. Brisou, Biofilms: Methods for Enzymatic Release of Microorganisms, CRC Press, Boca Raton, Florida, 1995.
[32] C.P.L. Grady, G.T. Daigger, H.C. Lim, Biological Wastewater Treatment, Marcel Dekker, New York, 1999.
[33] M.E. Davey, G.A. O'Toole, Microbiol. Mol. Biol. Rev. 64 (2000) 847.
[34] T.J. Beveridge, in: P. Actor, L. Daneo-Moore, M.L. Higgins, M.R.J. Salton, G.D. Shockman (Eds.), Am. Soc. Microbiol., Washington, DC, 1988, p. 3.
[35] D. Cozzi, P.G. Desideri, I. Lepri, J. Chromatogr. 40 (1969) 130.
[36] M.W. Mittelman, G.G. Geesey, Appl. Environ. Microbiol. 49 (1985) 846.
[37] R.J.C. McLean, D. Fortin, D.A. Brown, Can. J. Microbiol. 42 (1996) 392.
[38] T.A.M. Bridge, C. White, G.M. Gadd, Microbiology 145 (1999) 2987.
[39] G.M. Teitzel, M.R. Parsek, Appl. Environ. Microbiol. 69 (2003) 2313.
[40] A.B. Chmurny, E.J. Quintero, R. Kneer, US patent, 9830503, 1998.
[41] P.F.A.M. Römkens, L.A. Bouwman, G.T. Boon, Environ. Pollut. 106 (1999) 315.
[42] M.O. Elasri, R.V. Miller, Appl. Environ. Microbiol. 65 (1999) 2025.
[43] T. Ophir, D. Gutnick, Appl. Environ. Microbiol. 60 (1994) 740.
[44] W.W. Nichols, S.M. Dorrington, M.P.E. Slack, H. Walmsley, Antimicrob. Agents Chemother. 32 (1998) 518.
[45] A.C.C. Plette, M.F. Benedetti, W.H. Van Riemsdijk, Environ. Sci. Technol. 33 (1996) 4465.
[46] J.B. Fein, Chem. Geol. 169 (2000) 265.
[47] N. Yee, J. Fein, Geochim. Cosmochim. Acta 65 (2001) 2037.
[48] R.E. Martinez, F.G. Ferris, J. Colloid Interface Sci. 243 (2001) 73.
[49] R.E. Martinez, K. Pedersen, F.G. Ferris, J. Colloid Interface Sci. 275 (2004) 82.
[50] E.E. Emnova, R.L. Tate III, D. Gimenez, A. Dascualinc, S. Toma, O. Gojnetschi, I. Seniscovscaia, in: II International Symposium: Advanced Biological Technologies and their Impact on Economy "Natural Products: Technologies for their Capitalization in Agriculture, Medicine, and Food Industry", 2005, p. 128.
[51] J.M. Meyer, M.A. Abdallah, J. Gen. Microbiol. 107 (1978) 319.
[52] U. Beherens, M. Ringpfeil, Pat. 24763. DDR, WP 30h/72537, 1963.
[53] E.E. Emmova, L.D. Varbenets, V.N. VAsiliev, A.G. Ciocarlan, O.S. Brovarskaia, N.Ju. Caunova, O.G. Ganea, S.I. Toma, Bull. Moldovan Acad. Sci. – Life Sci. 1 (2007) 14.
[54] E.E. Emnova, A. Ciocarlan, N. Caunova, Ovidius University Annals of Chemistry, 17(2) (2007) 187.
[55] L.J. Bellamy, The Infrared Spectra of Complex Molecules, Chapman and Hall, London, 1975.
[56] S. Compte, G. Guibaud, M. Baudu, Process Biochem. 41 (2006) 815.
[57] D.V. Richmond, D.J. Fisher, Adv. Microbiol. Physiol. 9 (1973) 1.
[58] A. van der Wal, M. Minor, W. Norde, A.J.B. Zehnder, J. Lyklema, Langmuir 13 (1997) 165.
[59] A. Gélabert, O.S. Pokrovsky, J. Schott, A. Boudou, A. Feurtet-Mazel, J. Mielczarski, E. Mielczarsky, N. Mesmer-Dudons, O. Spalla, Geochim. Cosmochim. Acta 68 (2004) 4039.
[60] O.S. Pokrovsky, G.S. Pokrovski, A. Gélabert, J. Schott, A. Boudou, Environ. Sci. Technol. 39 (2005) 4490.
[61] A. Gélabert, O.S. Pokrovsky, J. Schott, A. Boudou, Geochim. Cosmochim. Acta 71 (2007) 3698.
[62] R.E. Martinez, O.S. Pokrovsky, J. Schott, E.H. Oelkers, J. Colloid Interface Sci. 323 (2008) 317.
[63] J.S. Cox, S. Smith, L.A. Warren, F.G. Ferris, Environ. Sci. Technol. 33 (1999) 4514.
[64] J.D. Allison, D.S. Brown, K.S. Novo-Gradac, K.S., MINTQA2/PRODEFA2, A Geochemical Assesment Model for Environment Systems. Version 3.0 Users Manual. U.S. EPA, Athens, GA, 1991.
[65] A.E. Martell, R.M. Smith, R.J. Motekaitis, NIST critically selected stability constants of metal complexes. Database software Version 3.0. Texas A&M University, College Station, TX, 1997.
[66] V.I. Slaveykova, K.J. Wilkinson, Environ. Sci. Technol. 36 (2002) 969.
[67] A. Smiejan, K.J. Wilkinson, C. Rossier, Environ. Sci. Technol. 37 (2003) 701.
[68] H.B. Xue, L. Sigg, Water Res. 24 (1990) 1129.
[69] C. Lamelas, F. Avaltroni, M. Benedetti, K.J. Wilkinson, V.I. Slaveykova, Biomacromolecules 6 (2005) 2756.
[70] C. Lamelas, M. Benedetti, K.J. Wilkinson, V.I. Slaveykova, Chemosphere 65 (2006) 1362.
[71] C.J. Tien, D.C. Sigee, K.N. White, J. Appl. Phycol. 17 (2005) 379.
[72] J. Ha, A. Gélabert, A.M. Spormann, G.E. Brown Jr., Geochim. Cosmochim. Acta 74 (2010) 1.
[73] J. Tourney, B.T. Ngwenya, J.W.F. Mosselmans, M. Magennis, J. Colloid Interface Sci. 337 (2009) 381.
[74] T. Boonfueng, L. Axe, N. Yee, D. Hahn, P.K. Ndiba, J. Colloid Interface Sci. 333 (2009) 439.
[75] I. Sokolov, D.S. Smith, G.S. Henderson, Y.A. Gorby, F.G. Ferris, Environ. Sci. Technol. 39 (2001) 341.
[76] C.J. Daughney, J.B. Fein, N. Yee, Chem. Geol. 144 (1998) 161.
[77] D. Borrok, J.B. Fein, Environ. Sci. Technol. 38 (2004) 5656.
[78] J. Tourney, B.T. Ngwenya, J. Colloid Interface Sci. (2010), doi:10.1016/j.jcis.2010.04.082.
[79] A. van der Wal, W. Norde, A.J.B. Zehnder, J. Lyklema, Colloids Surf. B: Biointerfaces 9 (1997) 81.
[80] R. De Philippis, M. Vincenzini, FEMS Microbiol. Rev. 22 (1998) 151.
[81] R. De Philippis, C. Sili, R. Paperi, M. Vincenzini, J. Appl. Phycol. 13 (2001) 293.
[82] H.N. Kim, Y. Hong, I. Lee, S.A. Bradford, S.L. Walker, Biomacromolecules 10 (2009) 2556.
[83] P.G. Burnett, H. Heinrich, D. Peak, P.J. Bremer, A.J. McQuillan, C.J. Daughney, Geochim. Cosmochim. Acta 70 (2006) 1914.
[84] J. Tourney, B.T. Ngwenya, J.W. Mosselmans, Chem. Geol. 247 (2008) 1.
[85] D. Borrok, J.B. Fein, Geochim. Cosmochim. Acta 68 (2004) 3043.
[86] S. Tsuneda, J. Jung, H. Hayashi, H. Aikawa, A. Hirata, H. Sasaki, Colloid Surf. B 29 (2003) 181.
[87] O. Braissant, A.W. Decho, C. Dupraz, C. Glunk, K.M. Przekop, P.T. Visscher, Geobiology 5 (2007) 401.
[88] A. Gélabert, O.S. Pokrovsky, J. Viers, J. Schott, A. Boudou, A. Feurtet-Mazel, Geochim. Cosmochim. Acta 70 (2006) 839.